Aragonite Formation in the Chiton (Mollusca) Girdle

by **Keren Treves**, **Wolfie Traub**, **Steve Weiner**, and **Lia Addadi***

Department of Structural Biology, Weizmann Institute of Science, Rehovot, Israel 76100

Dedicated to Professor *Jack D. Dunitz* on the occasion of his 80th birthday

In the chitons (Polyplacophora, Mollusca), the body is not entirely protected by the shell. Mineralized spicules or scales often, but not always, decorate the exposed part of the girdle. Here, we report a study on the composition and ultrastructural organization of these mineralized skeletal parts in four different chiton species. In all specimens, the mineral component (97–98 wt-%) is aragonite, and the organic matrix (2–3 wt-%) consists of highly glycosylated proteins. X-Ray diffraction and scanning electron microscopy show that the organic matrix fibers are aligned, morphologically and crystallographically, with the prismatic aragonite crystals. Matrix and mineral are thus clearly related. The matrix–mineral composite bundles are, however, assembled in the various skeletal parts examined with widely different degrees of alignment and order. In the same organism, the crystals are aligned within a range of $\pm 15^{\circ}$ in one type of spicule, while they are randomly oriented in another type. The wide heterogeneity in shape, density, and ultrastructure suggests that the girdle mineralized tissues do not fulfill a fundamental role necessary for the survival of the organism. This, together with the lack of chitin in the organic matrix, supports the hypothesis that they evolved separately from the other chiton mineralized tissues, namely the shell plates and teeth.

Introduction. – Calcium carbonate minerals are formed in vast amounts by many different organisms [1]. The crystals generally form in matrix frameworks, and their orientations, polymorph type, and morphologies are influenced by the matrix and by the environment in which they grow. They are, thus, the focus of much research in the field of biomineralization aimed at understanding the manner in which control is exerted over the biomineralization process.

Calcium carbonate crystallizes in three anhydrous polymorphs; calcite, aragonite, and vaterite [2]. The most-common polymorphs formed by organisms are calcite and aragonite, and this is under strict genetic control. Calcite is the most stable form at ambient temperatures and pressures. Calcite formation at ambient temperature from pure water or from buffered solutions not containing Mg is both thermodynamically and kinetically favored. The formation of aragonite is, however, favored in the presence of Mg in high concentrations relative to Ca. Interestingly, the density of aragonite (2.93 g/cm^3) is higher than that of calcite (2.71 g/cm^3), such that aragonite is more stable than calcite at very low temperatures, close to absolute zero. Magnesium ions are not incorporated in the denser lattice of aragonite as a solid solution, in spite of Mg^{2+} being a smaller ion than Ca^{2+}. This occurs presumably because magnesium has a tightly bound hydration shell, and its removal during crystal growth is energetically unfavorable. In contrast to aragonite, Mg^{2+} ions may be incorporated inside the calcite lattice. The presence of Mg in the calcite lattice, as may be expected, destabilizes it, such that at 12 mol-% Mg content, calcite becomes less stable than aragonite [3][4]. The distribution constant of Mg between water and calcite at ambient temperatures

and pressures is around 0.06, such that aragonite precipitation is favored from solutions that contain Mg^{2+}/Ca^{2+} at a ratio of >2. This corresponds approximately to the Mg^{2+}/Ca^{2+} ratio in freshwater, while, in seawater, Mg/Ca^{2+} is greater than 5 (Ca^{2+} *ca.* 10mM, Mg^{2+} *ca.* 50mM). Consequently, calcite is not stable, and aragonite precipitates in sea water [4]. This is the reason why some organisms, such as certain algae, that induce precipitation of calcium carbonate on their external surface, form aragonite in seawater and calcite in freshwater [5][6]. The process whereby these organisms deposit minerals has been referred to as 'biologically induced mineralization', suggesting that the organism induces crystal deposition, but has no further control over its formation [7].

More commonly, the control that is exercised by the organism goes well beyond simple induction of mineral deposition, and extends to all the properties of the crystals deposited, including polymorphism, orientation, morphology, and size. The extracellular ionic environment where the mineral forms is established by specialized tissue cells and controlled by them. Thus, the two polymorphs, calcite and aragonite, are often deposited side-by-side by the same organism, but always in different mineralized compartments [1]. Many examples of the latter mineralization strategy are known in mollusk shells [8].

What, then, is the advantage of using aragonite rather than calcite or *vice versa*? An overview of biological mineralization (see, *e.g.*, micrographs by *Carter* [9]) supports the notion that calcite is more advantageous than aragonite as a building material. Calcite single crystals are sculpted by organisms into fantastically convoluted morphologies, and may reach sizes of up to several centimeters. In the skeletal elements of echinoderms, *e.g.*, entire spines or test plates are composed of single crystals of calcite [10]. In contrast, aragonite appears to have morphology that is much more difficult to manipulate. With a few consipicuous exceptions, such as the well-studied mollusk shell nacre, biogenic aragonite crystals are in the μm size range, and grow as needles or prisms elongated in the direction of the *c* axis. Wherever larger skeletal parts are built of aragonite, biological mineralization utilizes the strategy of growing tightly packed polycrystalline ensembles, where the single crystals may or may not be accurately oriented relative to their crystallographic axes [11].

The present study focuses on the ultrastructure of a very poorly documented mollusk mineralized tissue, the mineralized girdle parts of the Polyplacophora or chitons, Mollusks are classified into seven different taxonomic classes, six of which are shell-bearing: the Bivalvia, Gastropoda, Cephalopoda, Scaphophoda, Monoplacophora, and Polyplacophora. The Aplacophora do not have a shell, but may have spicules embedded in their mantle tissue [12]. All the shells are composite materials formed of mineral deposited inside an organic matrix framework. The organic matrix in all mollusk shells examined to date comprises chitin as an essential component of the framework molecules [1]. The chitons have a shell composed of eight aragonitic plates, hence the name polyplacophora (= bearer of many plates). The shell covers only part of the body, while the remaining part of the body, the girdle, may be protected by spicules, scales, or may not be mineralized [12]. We were attracted to the study of these spicules and scales because their construction blueprint, although under complete cellular control, appears to be substantially different from what has been observed in the chiton shell plates and the mineralized teeth, as well as most other mineralized parts of other mollusks.

In the one published study of spicule mineralization in the Polyplacophora, *Haas* [13] described spicule formation as an initially intracellular process. Further growth of the spicule occurs inside a crystal chamber composed of organic macromolecules secreted by a number of cells surrounding the spicule. The spicule growth is, thus, under total cellular control all stages, including the initial intra-cellular stage and the later extra-cellular maturation stage. Here, we focus on the structure and composition of the mature mineralized product of the girdle mineralization process.

Results. – Four different genera of chitons were examined and compared: *Acanthopleura uaillantii* (*Fig. 1*), *Acanthopleura spinigera, Nuttalina fluxa,* and *Ischnochitonina* sp. The girdles of the first three are decorated by spicules with a typical sturdy elongated shape (*Fig. 2, a–d*). *A. uaillantii* has bands of light and dark spicules, which are different in color, and these were examined separately. In contrast to the other species, *Ischnochitonina* sp. does not have girdle spicules, but tightly packed overlapping scales that cover the girdle (*Figs. 2, e* and *f*). The mineral and the mineral organization within the spicules were first characterized by IR spectroscopy, scanning electron microscopy, and X-ray diffraction.

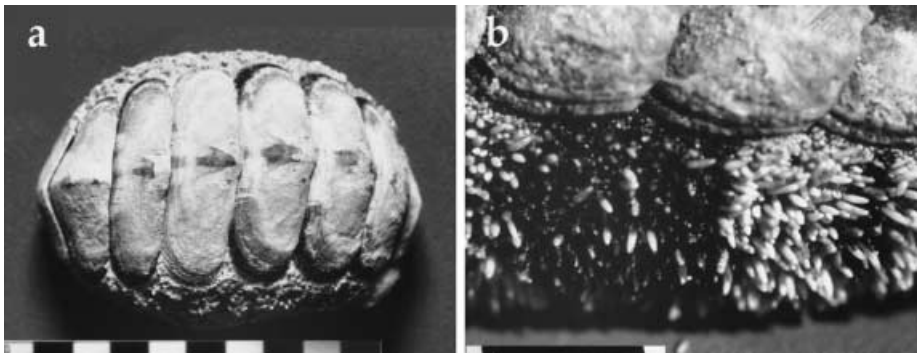

Fig. 1. *The chiton* A. uillantii. Note the dorsal plates, forming the shell, and the girdle, decorated by spicules, surrounding them. b) *Close-up on a part of girdle, showing the bands of white and black spicules.* Scale bar: 5mm.

The only mineral component in the spicules and plates is aragonite, based on X-ray diffraction and IR spectroscopy. Individual spicules or scales behave under polarized light and X-ray diffraction as polycrystalline materials. Indeed, broken sections of the spicules observed in the scanning electron microscope have a morphology characteristic of polycrystalline aragonite. The single crystallites appear as discrete, elongated prisms, a few μm in length and are of sub-μm thickness. The individual crystallites are tightly packed in bundles. Within a bundle, the elongated prisms have their long axes (the *c* axis of aragonite) aligned, thus forming a compact material. In *A. uaillantii* white spicules, the bundles are haphazardly oriented one relative to the other (*Fig. 3, a*). In *Ischnochitonina* sp. scales, the bundles appear to be aligned with respect to the scale morphological axes (*Fig. 3, b* and *c*). The rows of bundles themselves do not, however, maintain a consistent orientation, as they follow the rounded morphology of the scale. In contrast to the two previous cases, in *A. spinigera* spicules (*Fig. 3, d*), *A. uaillantii* black spicules (*Fig. 3, e*), and *N. fluxa* spicules (*Fig. 3, f*), the crystals display a preferred

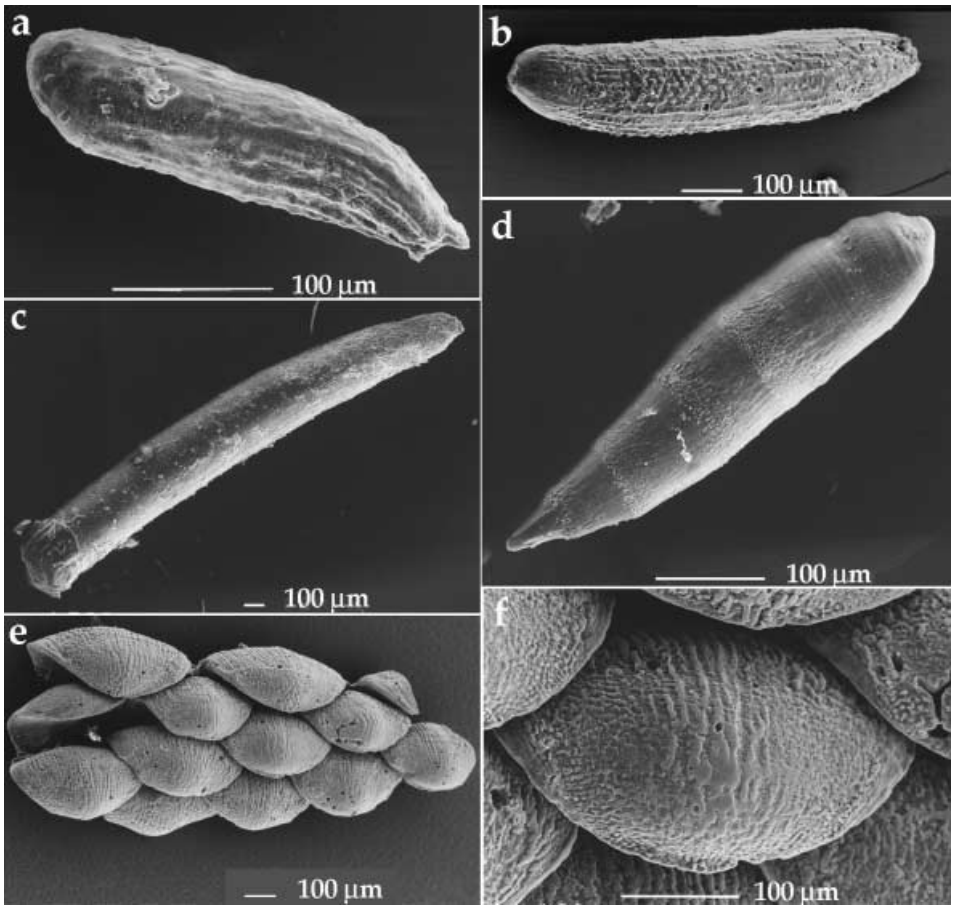

Fig. 2. *Scanning electron micrographs of girdle mineralized hard parts of chitons. a*) *A. uaillanti* white spicule; *b*) *A. uaillanti* black spicule; *c*) *A. spinigera* spicule; *d*) *Nuttalina fluxa* spicula; *e*) *Ischnochitonina sp.* plates; *f*) *Ischnochitonina sp.*, enlargement of one plate. Scale-bars are different and are thus specified in each micrograph.

orientation parallel to the long dimension of the spicule. The crystals fan out over an angle of not more than 30°, starting from one end of the spicule and spreading out from the center of the spicule.

X-Ray-diffraction patterns were collected from single spicules or scales with a flat plate micro-camera, with the X-ray beam perpendicular to the long axis of the specimen (or to the median axis for the scales). The diffraction patterns are typical of aragonite in all samples. The (002) reflection, corresponding to a *d* spacing of 2.87 Å along the *c* axis, is particularly useful for mapping crystal alignment. The crystals of *A. uaillantii* white spicules have a random orientation, as indicated by the presence of complete diffraction rings (*Fig. 4, a*). The X-ray-diffraction pattern of *Ischnochitonina* sp. shows some evidence of preferred orientation, as indicated by broad (002) arcs that subtend an angle of *ca.* 45° (*Fig. 4, b*). Note that a substantial amount of material

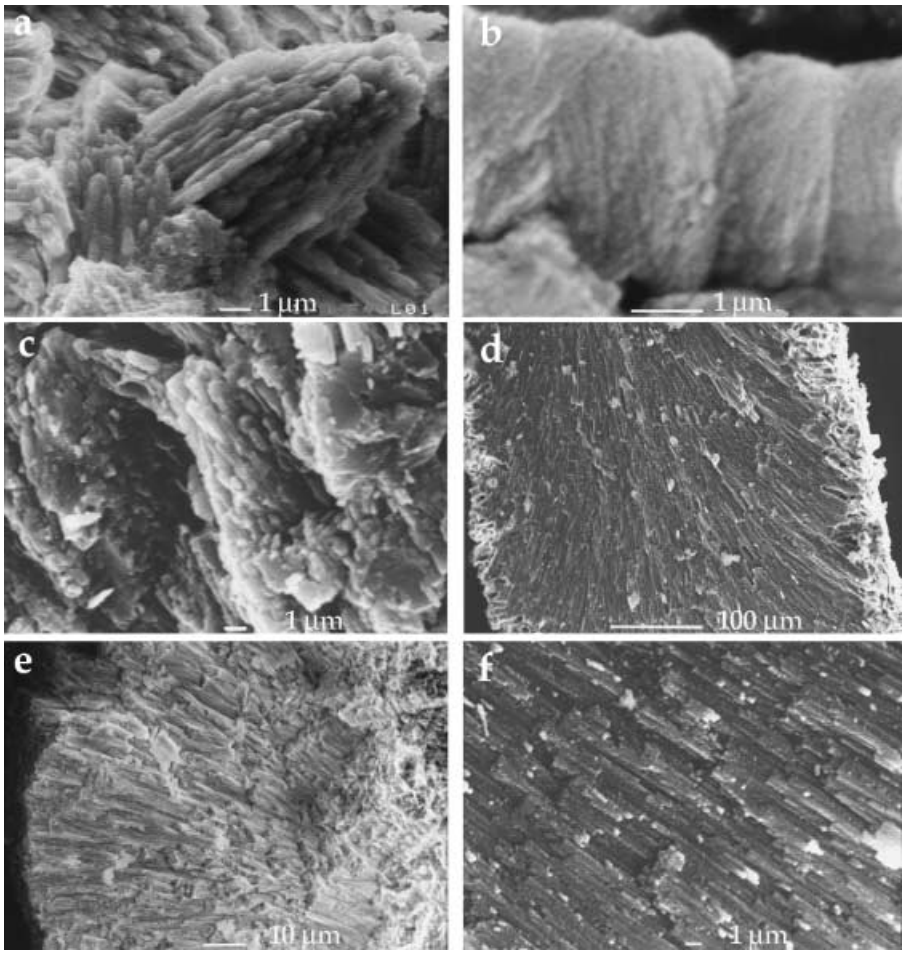

Fig. 3. *Scanning electron micrographs of fractured sections of girdle mineralized hard parts of chitons. a*) *A. uaillantii* white spicule, cross section; *b*) *Ischnochitonina sp* scale, section parallel to the ventral surface; *c*) *Ischnochitonina sp* scale, cross section; *d*) *A. spinigera* spicule, longitudinal section; *e*) *A. uaillantii* black spicule, cross section; *f*) *N. fluxa* spicule, longitudinal section. Scale-bars are different and are thus specified in each micrograph.

diffracts outside the arcs. In addition, the diffraction pattern is composed of sharp spots, rather than a continuous arc. Each reflection spot may be due to relatively large single crystals within each crystal bundle, or to very good alignment of many crystals within individual bundles. The diffraction patterns of *A. spinigera* spicules and *A. uaillantii* black spicules show a higher degree of alignment, with the (002) arcs subtending an angle of only 30° (±15° around the median) and practically no diffraction outside the arcs (*Fig. 4, c* and *d*).

The mineral–organic matrix relations were investigated to gain more insight into the mode of mineral formation. The mineral component was removed by decalcification with an anion-exchange resin, or by dissolution in diluted HCl [14]. All these

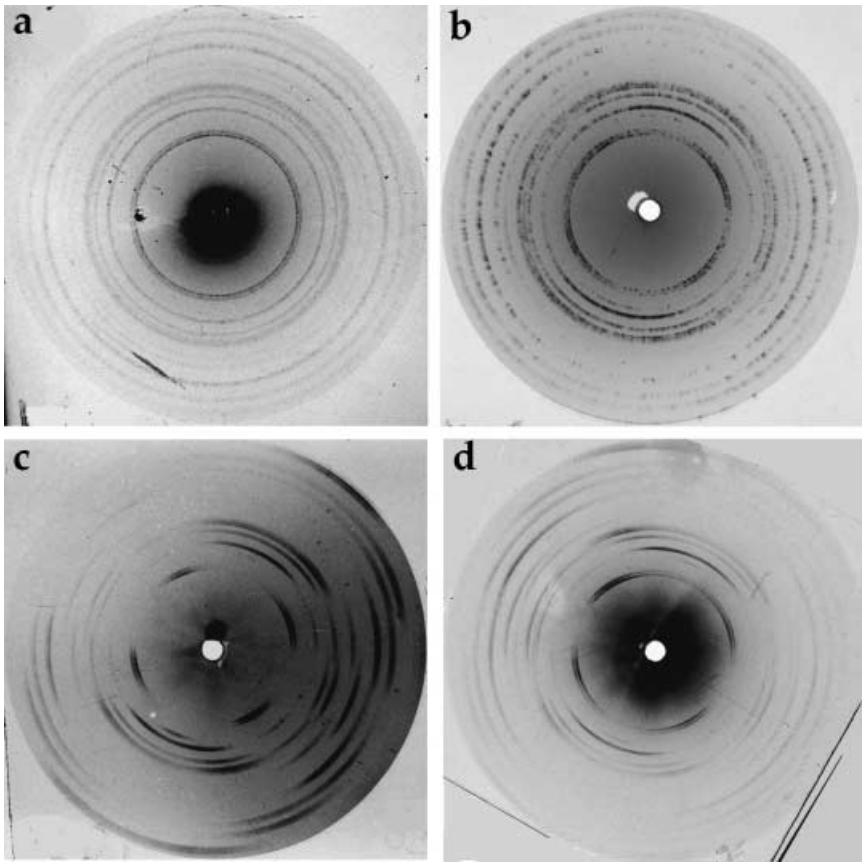

Fig. 4. *X-Ray-diffraction patterns from girdle mineralized hard parts of chitons.* The photographs were taken with the X-ray beam perpendicular to the long morphological axis of the spicules and to the median axis of the plates. *a*) *A. uaillantii* white spicule; *b*) *Ischnochitonina sp.* plate; *c*) *A. spinigera* spicule; *d*) *A. uaillantii* black spicule.

treatments leave a conspicuous envelope of insoluble matrix, supported by a massive internal network of fibers. These form the framework within which mineralization occurs. In addition, small amounts of macromolecules are released in a H_2O-soluble form. Information about the relative amounts and the composition of the organic matrices associated with the different spicules and scales decalcified with HCl is reported in the *Table*. The overall compositions of the spicules and scales are rather similar, including both white and black spicules of *A. uaillantii*. The Asx content of the acid-soluble fraction is greater than that of the acid-insoluble fraction, implying that the former fraction contains a higher proportion of Asx-rich proteins. The high Gly and Ala contents may be an indication of the presence of proteins similar to silk in both fractions. Silk is a major component of the insoluble fractions of many mollusk shell organic matrices [1][15]. Surprisingly, the insoluble matrix of the spicule does not appear by IR spectroscopy (*Fig. 5, a*) to contain the typical spectrum of chitin, which is

Table 1. *Amino Acid Composition* (mol-% of total protein) *and Organic Matrix Content* (wt-% of mineral) *in the H_2O-Soluble* (sol) *and Insoluble* (insol) *Matrix Fractions Obtained after Demineralization with Diluted HCl of the Girdle Mineralized Hard Parts of* A. uaillantii, A. spinigera, *and* Ischnochitonina *sp.*

Amino acid	*A. uaillantii*				*A. spinigera*		*Ischnochitonina* sp.	
	white spicule		black spicule		spicule		scale	
	sol	insol	sol	insol	sol	insol	sol	insol
Asx	20.7	10.8	19.7	9.4	14.3	12.3	18.2	11.4
Gly	26.6	21.3	27.6	25.7	21.5	15.7	19.1	21.0
Ala	7.4	9.2	9.5	9.4	8.3	7.5	7.6	7.7
Acidic[a])	34.0	19.7	29.7	21.4	26.3	21.0	33.1	22.6
Polar[b])	53.7	44.3	50.1	43.7	45.9	45.9	57	47.7
Hydrophobic[c])	47.1	60.9	54.6	60.7	56	58.4	46.4	57.6
Total protein	0.1	0.13	0.15	0.11	0.16	0.13	0.15	0.16
Organic matrix		2.3		3.0		3.0		2.0

[a]) Acidic amino acids: Asx, Glx. [b]) Polar amino acids: Thr, Ser, Lys, His, Arg, Tyr, Cys. [c]) Hydrophobic amino acids: Gly, Pro, Ala, Cys, Val, Met, Ile, Leu, Tyr, Phe.

clearly present as the major component in the shell plates from the same species (*Fig. 5, b*). Chitin is common in mollusk shell matrices [16]. The insoluble matrices of the spicules appear to be composed, in all samples, of heavily glycosylated proteins. These form a meshwork of fibers that are morphologically very different one from the other in the samples studied (*fig. 6, a – d*). Specifically, *A. uaillantii* white spicules and *Ischnochitonina* sp. scale matrices appear in dried samples as lamellae, and do not have a preferred spatial orientation (*Fig. 6, a* and *b*). In contrast, the fibers comprising the matrix of *A. spinigera* spicules (*Fig. 6, c*) and *A. uaillantii* black spicules (*Fig. 6, d*) form a meshwork with a clearly defined preferred orientation.

A. spinigera spicules appear to be the ones that have the highest alignment of the aragonite crystals and of the framework matrix. Moreover, we noted that the X-ray

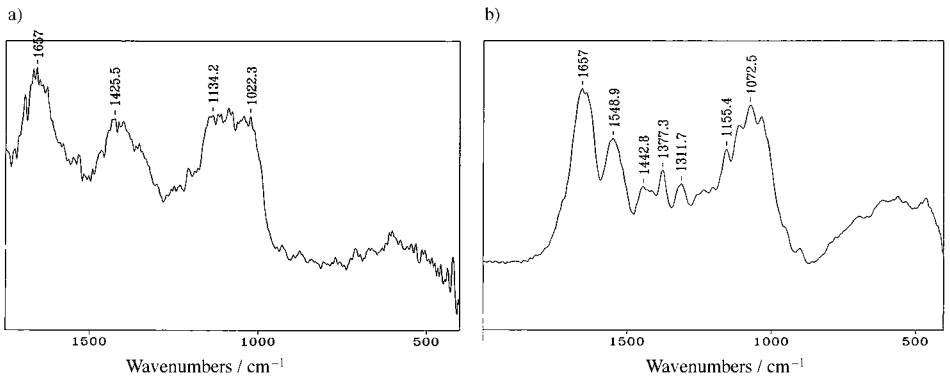

Fig. 5. *IR Spectra of the ensemble of H_2O-insoluble macromolecules forming the organic matrix of the mineralized tissue, obtained after dissolution of the mineral from. a*) *A. spinigera* spicules; *b*) *A. spinigera* shell plates. The spectrum *b* is typical of chitin.

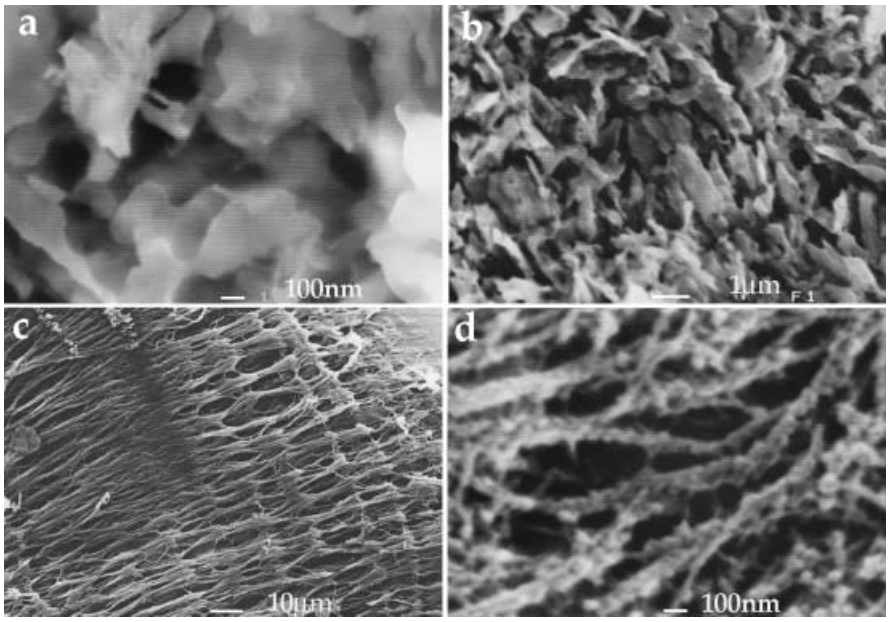

Fig. 6. *Scanning electron micrographs of demineralized, fixed, and critical-point dried girdle hard parts of chitons. a*) *A. uaillantii* white spicule matrix; *b*) *Ischnochitonina* sp. scale matrix; *c*) *A. spinigera* spicule matrix; *d*) *A. uallantii* black spicule matrix. Scale-bars are different and are thus specified in each micrograph.

diffraction pattern of the spicules shows additional arcs at the center of the aragonite diffraction pattern. These have the characteristic blurred appearance of diffraction from organic fibers, and their positions correspond to *d* spacings too long to be attributed to aragonite. If these reflections are considered *vis-à-vis* those of the mineral, information can be obtained on the orientation of the crystals relative to the matrix. To obtain a better diffraction pattern from the organic material, spicules were partially dissolved, and, indeed, these diffraction patterns show much clearer components from the organic matrix fibers (*Fig. 7*). The matrix reflections include arcs and dots. The arcs are parallel to the (002) reflection of the aragonite crystals, while the dots are well-aligned with the (111) and the (021) reflections of aragonite. There is, thus, a well-defined spatial relationship between matrix and mineral. Surprisingly, these reflections do not correspond to chitin, or to any identifiable fiber structure. Diffraction patterns due to organic material were also observed for *A. uaillantii* black and white spicules. In the white spicules, this consists of full circles, indicating total lack of orientation of the organic matrix, while, in the black spiucles, the diffraction pattern resembles that of *A. spinigera*.

We can, thus, conclude that the degree of orientation of the crystals, deduced from X-ray-diffraction as well as from the SEM examination of the mineral ultrastructure, matches well the degree of orientation of the matrix, deduced from both SEM of the demineralized spicules and from X-ray-diffraction patterns of etched spicules. Matrix and mineral are clearly related.

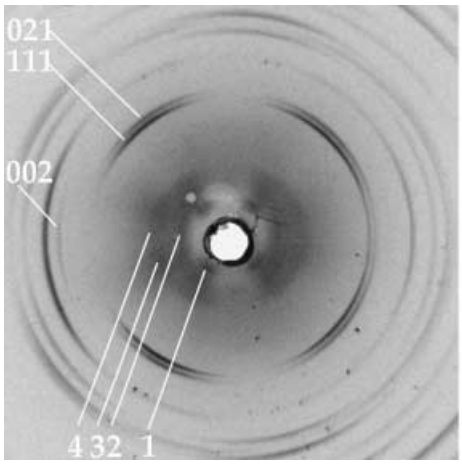

			I	*d* / Å	*hkl*
a)			*vs*	3.40	111
			s	3.27	021
			w	2.87	002
b)	1	dots	*s*	11.5	
	2	arcs	*s*	9.7	
	3	dots	*m*	6.9	
	4	arcs	*m*	5.9	

Fig. 7. *X-Ray-diffraction photograph of an etched* A. spinigera *spicule.* Diffraction from both mineral and matrix can be detected. Enlarged diffraction pattern of the innermost range. The matrix diffraction, marked by numbers, is more diffuse than the mineral diffraction, and corresponds to longer *d* spacings (*i.e.*, to shorter measured distances in the diffraction photograph). The *c* axis is horizontal. Table of the significant reflections and corresponding *d* spacings; a) mineral; b) matrix.

Discussion. – We showed here that the girdle spicules and scales are all composed of aragonite, confirming earlier studies [17]. The crystals within the spicules and scales are organized to different extents. Most surprising is the observation that the organization of the crystals in the black and white spicules from the same tissue is so different. This is rare in the filed of biomineralization. We also show that there is a well-defined spatial relationship between matrix and crystals, implying that the matrix somehow controls crystal nucleation. Less obvious is the extent to which the biological environment controls the growth of the aragonite crystals. Furthermore, the absence of chitin in the spicule matrix shows that the spicule biomineralization process is significantly different from that of the shell plates of the chiton itself and from mollusk shells in general, as chitin fulfills an important scaffolding function in shell formation [18]. We note that the amount of organic matrix, 2–3% by weight of dry mineral, is higher than in other mollusk mineralized tissues, which is normally $<1\%$ [19]. The amounts of protein in the spicules and scales, on the other hand, are remarkably low, between 0.07 and 0.23%, indicating that most of the matrix consists of polysaccharides. The organic material also forms a dense, massive meshwork of fibers or lamellae, very different from the framework commonly observed in mollusk shells. All the above evidence indicates that the chiton girdle mineralized parts have mechanisms of formation different from those of the other mineralized parts of the same organisms and probably of other mollusks as well. It is, thus, of interest to try to better understand the modes of control involved in girdle spicule and scale formation.

A key reference point is the comparsion of aragonite crystals formed abiologially with those present in the girdle spicules and scales. *Fig. 8, a* shows an example of aragonite crystals that formed abiologically in the Dead Sea and is now deposited in the sediments of the Lisan Formation. They are all prism-shaped and are present as

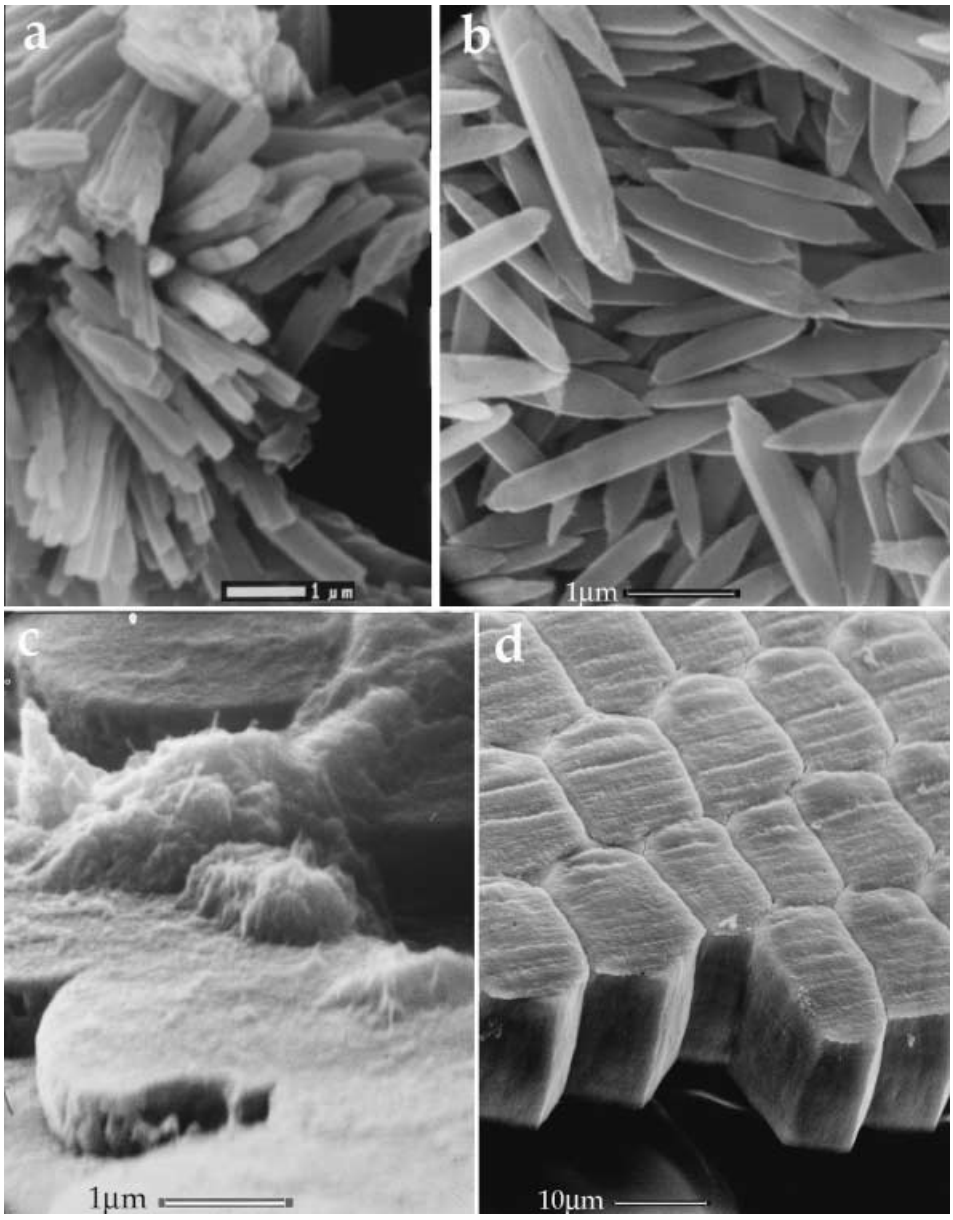

Fig. 8. a) *Crystals of aragonite that precipitated in the Dead Sea without any biogenic influence and are now part of the sediments of the Lisan formation.* b) *Crystals of aragonite deposited by the squid* Symplectoteuthis onlaniensis (also a mollusk) *as part of its gravity-sensing apparatus.* c) *Growing aragonite tablets deposited by the mollusk* Neottrigonia margaritacea *in the nacreous layer of the shell.* Needle-shaped crystals grow first along their *c* axes, and only later expand in the direction of *a* and *b*. d) *Aragonitic prisms from the shell of* Neopilina hyalina. Micrographs *b – d* were from the late *H. A. Lowenstam*.

bundles, properties that closely resemble the basic ultrastructural motif found in the spicules and scales. This points to little control being exercised over crystal growth, despite the fact that the biogenic crystals form inside an organic matrix, and the matrix components are aligned with the crystallographic axes.

Fig. 8, b is an example of similar aragonitic prisms produced by a squid, which also belongs to the mollusk phylum. These aragonitic crystals are part of the gravity-sensing apparatus. In fact, a perusal of the literature shows that biogenic aragonite in the form of prism-shaped crystals arranged in bundles is rather common in mollusks [20] and in other animal phyla, such as coral skeletions and vertebrate otoliths [1][9]. Less common among the mollusks are biogenic aragonite crystals with shapes that are not thin elongated prisms. *Fig. 8, c* and *d* show perhaps two of the most familiar examples of aragonite crystals from mollusks; nacre and aragonitic prisms respectively. The nacre tablets are, indeed, twinned crystals of aragonite, whereas the prisms may be single crystals, but usually are composed of many small prism-shaped crystals of aragonite [21]. In fact the prisms of Neopilina (*Fig. 8, d*), are multicrystalline [21]. Only in the nacreous aragonitic tablets are the *c* axes aligned with the short dimension of the crystal, *i.e.*, perpendicular to the thickness. We have observed that, during the formation of a new tablet, needle-shaped crystals grow first along their *c* axes (*Fig. 8, c*), and only after they have reached their maximum length defined by the prepositioned organic matrix do they grow laterally along their *a* and *b* axes. We thus conclude that, in mollusks and other mineralized tissues, aragonite, in contrast to calcite, tends to maintain its normal prism-shaped crystal morphology, and only exceptionally does the biological environment of crystal growth override this natural propensity. The chiton spicules are not an exception in this respect.

The spicules and scales conceivably serve for protection of the exposed soft tissues. They probably do not fulfill a fundamental role on which the organism relies for survival: this we surmise from their wide variability in shape, density, and ultrastructure, including the total lack of girdle mineralized tissues in some genera. The results of our study suggest that the girdle-mineralized tissues evolved separately from the mineralized tissues of the shell and teeth, both of which form in a chitinous organic matrix framework. The girdle-mineralized deposits are, thus, interesting subjects for investigation, both in terms of evolution, and for the understanding of basic biomineralization mechanisms.

Experimental Part

General. Specimens of *Acanthopleura uaillantii* were collected alive in the Sinai peninsula, Nuweiba, Egypt. They were frozen and stored at -20° without further treatment until used. Specimens of what we suspect are *Ischnochitonina* sp. were collected alive on the south coast of Australia. The species identification was not possible. They were washed in H_2O and then briefly in EtOH. The girdles were removed, dried, and stored at r.t. until used. Specimens of *Acanthopleura spinigera* were collected alive in Palau, South Pacific, and stored dry at r.t. until used. Specimens of *Nuttalina fluxa* were collected alive on the coast of Santa Barbara, California, USA. They were flash frozen and stored at -20° without further treatment until used. The girdles were dissected out of the tissue, and the spicules were mechanically removed, immersed in H_2O, and treated for few min with a *Branson* ultrasonic cleaner to remove adhering external tissue. They were finally extensively washed in H_2O, and examined without further chemical treatment.

Scanning Electron Microscopy. Whole or broken spicules were attached to aluminum stubs by carbon-coated adhesive tape, sputter-coated with gold, and examined in a *Jeol 6400* scanning electron microscope. The etched specimens were sectioned and fixed with 4% HCHO, 0.5% *N*-cetylpyridinium chloride overnight. The fragments were then etched in 1:1 mixture of the above fixative soln. containing 0.5M ethylenediaminetetraactic

acid (EDTA) at pH 8.0 at r.t. for various times (5, 15, 30, 60 min and overnight) and washed. The samples were then critical point dried (*PELCO CPD-2*) after being dehydrated in an EtOH gradient, and prepared for examination as described above.

X-Ray Diffraction. X-Ray-diffraction patterns were obtained with a *Norelco Chesley* flat-plate micro-camera, with CuK_α radiation, 32 mV, 20 mA, and 5–15 h exposures. The specimen/film distance was 12 mm. The specimens were aligned with their long morphological axes (or the median axis for the scales) perpendicular to the X-ray beam.

Demineralization and Matrix Analysis. Dry, cleaned spicules and scales were ground in a mortar and weighed. The fine powder was suspended in H_2O. Stoichiometric amounts of 10.4M HCl were added dropwise (1 drop/5 min) under agitation. Care was taken to maintain the pH above 6 during the demineralization procedure. The final pH was *ca.* 6.5. After complete demineralization, the soln. was dialyzed exhaustively (*Spectra-Por 3* dialysis membranes), the soluble material was separated from the insoluble matrix by centrifugation (3000*g*, 4 min), and washed. The soln. was lyophilized and stored at 4°. Alternatively, demineralization was performed with an ion-exchange resin according to the procedure of *Albeck et al.* [14]. Amino acid analyses were performed with an automatic amino acid analyzer (*HP 1090 Amino Quant* with OPA detection) on weighed aliquots. The total protein yields were used to calculate the protein contents of the samples.

IR Spectrometry was performed using KBr pellets at 4-cm^{-1} resolution with an FTIR spectrometer (*MIDAC Corporation*, Costa Mesa, CA, USA).

S. W. is the incumbent of the Dr. *Walter* and Dr. *Trude Burchardt* Professional Chair of Structural Biology, and *L. A.* is the incumbent of the *Dorothy and Patrick Gorman* Professiorial Chair of Biological Ultrastructure. *L. A.* gratefully acknowledges support of her research by the *Ziegler* family trust.

REFERENCES

[1] H. A. Lowenstam, S. Weiner, 'On Biomineralization', Oxford University Press, New York, 1989.
[2] F. Lippmann, 'Sedimentary Carbonate Minerals', Springer Verlag, Berlin, 1973.
[3] K. E. Chave, K. S. Deffeyes, P. K. Weil, R. M. Garrels, M. E. Thompson, *Science* **1962**, *157*, 33.
[4] A. Katz, *Geochim. Cosmochim. Acta* **1973**, *37*, 1563.
[5] A. P. Vinogradov, 'The Elementary Chemical Composition of Marine Organisms', Sears Foundation for Marine Research II, Yale University, New Haven, 1953.
[6] M. A. Borowitzka, in 'Biomineralization in Lower Plants and Animals', Eds. B. S. C. Leadbeater, R. Riding, Claredon Press, Oxford, 1986.
[7] H. Lowenstam, *Science* **1981**, *211*, 1126.
[8] N. Watabe, in 'The Mollusca', Eds. K. M. Wilbur, E. R. Trueman, M. R. Clarke, Academic Press, New York, 1988.
[9] 'Skeletal Biomineralization: Patterns, Processes and Evolutionary Trends', Ed. J. G. Carter, Van Nostrand Reinhold, New York, 1990.
[10] D. M. Raup, *J. Geol.* **1959**, *67*, 661.
[11] L. Addadi, S. Weiner, *Angew. Chem., Int. Ed.* **1992**, *31*, 153.
[12] 'Treatise on Invertebrate Paleontology. Part 1. Mollusca', Ed. R. C. Moore, University Press of Kansas, 1960.
[13] W. Haas, in 'The Mechanisms of Mineralization in the Invertebrates and Plants: Symposium', Eds. N. Watabe, K. M. Wilbur, University of South Carolina Press, Columbia, 1976.
[14] S. Albeck, S. Weiner, L. Addadi, *Chem.–Eur. J.* **1996**, *2*, 278.
[15] S. Sudo, T. Fujikawa, T. Nagakura, T. Ohkubo, M. Sakaguchi, K. Tanaka, K. Nakashima, T. Takahashi, *Nature* **1997**, *387*, 563.
[16] C. Jeunieux, 'Chitine et Chitinolyse', Masson, Paris, 1963.
[17] V. Cornish, P. F. Kendall, *Geol. Mag.* **1888**, *5*, 66.
[18] Y. Levi-Kalisman, L. Addadi, S. Weiner, *J. Struct. Biol.* **2001**, *135*, 8.
[19] P. E. Hare, P. H. Abelson, 'Amino acid composition of some calcified proteins', in 'Carnegie Institute of Washington Year Book 64', Washington, 1965, p. 223–232.
[20] K. Bandel, in 'Skeletal Biomineralization: Patterns, Processes and Evolutionary Trends', Ed. J. G. Carter, Van Nostrand Reinhold, New York, 1990, p. 117–134.
[21] J. G. Carter, G. R. Clark, in 'Mollusks: Notes for a Short Course Organized by D. J. Bottjer', Ed. T. W. Broadhead, 1985, p. 50–71.

Received January 31, 2003